

Autonomous Decentralized Control of a Quadruped Locomotion Robot using Oscillators

Katsuyoshi Tsujita, Ahmet Onat, Kazuo Tsuchiya and Yousuke Kawano
Dept. of Aeronautics and Astronautics
Kyoto University
Yoshida-honmachi, Sakyo-ku, Kyoto 606-8501, Japan

Abstract

This paper deals with the design of a control system for a quadruped locomotion robot. The proposed control system is based on the bottom up approach and it is composed of a leg controller and a gait pattern controller describing a hierarchical architecture. The leg controller drives the actuators at the joints of the legs using high-gain local feedback control. It receives the commanded signal from the gait pattern controller. The gait pattern controller, on the other hand, involves nonlinear oscillators. These oscillators interact with each other through the signals from the touch sensors located at the tips of the legs. The control system repeatedly moves the legs in predefined motion patterns, synchronizing the motion with the signals from the touch sensor. It also adaptively stabilizes the phase differences between the motions of the legs. The performance of the proposed control system was verified by numerical simulations and hardware experiments.

1 Introduction

Locomotion is one of the basic functions of a mobile robot. Using legs is one of the strategies for accomplishing locomotion. Although simpler forms of locomotion such as wheels can be easier to design and control, using legs for locomotion allows the robot to move on rough terrain, and therefore improves access to many locations. Therefore, a considerable amount of research has been done on motion control of legged locomotion robots. This paper deals with the motion control of a quadruped locomotion robot.

Several gait patterns can be considered for quadruped locomotion robots. The gait pattern in which any combinations of three legs of the robot support the main body at any instant during locomotion is called *walk* pattern. For low velocities in which the inertia effect is small enough, the walk pattern is statically stable in terms of the dynamics of the robot mechanism. However, if the velocity of locomotion increases, the locomotion of the robot becomes unstable. On the other hand, *trot* pattern is a gait pattern

in which two legs of the robot support the main body at any instant during locomotion. This pattern is statically unstable, and it is difficult for the robot to sustain a stable locomotion at low velocities. However, at higher velocities, the robot can sustain stable locomotion with the trot pattern by using its inertia effectively. Designing a control system for realizing stable locomotion by changing the gait pattern to adapt to the desired velocity or to the properties of the environment is a subject of the research in motion control of the quadruped locomotion robot. In order to design the locomotion controller, we need to design the gait patterns and the motion controller. For designing the gait patterns, we first determine the nominal gait patterns and the trajectories of the legs to realize the nominal gait patterns. The motion controller is designed to realize the nominal motions of the legs.

There are two ways to design the control system of the robot, *top down approach* and *bottom up approach*. The top down approach is based on control theory. The design of the trajectories of the legs and the gait patterns are implemented through optimization based on the inverse model of the robot. The motion controllers are designed based on the linearized model. In this system, nonlinear dynamics such as Coriolis force are eliminated by using the computed torque method, the nonlinear feedback method, etc [1]. The top down approach designs the control system based on the mathematical model of the robot and that of the environment. Therefore, control systems designed in this way are not always robust. On the other hand, the bottom up approach to design the control system is based on the animal behavioral sciences [2] ~ [4]. The animal behavioral science teaches us that the control systems of animals make the legs repeat a forward and backward motion periodically if the legs have no mechanical interaction with the ground. It also teaches us that animals have touch sensors at the tips of the legs and motions of the legs interact with each other through the input signals from the touch sensors. These interactions modify the phase relations of periodic motions of the legs appropriately. As a result, a gait pattern that can satisfy the require-

ments of the locomotion velocity or the properties of the environment emerges. The bottom up approach design is performed in the following way: First, we introduce nonlinear oscillators in the leg controllers and determine the periodic motion of the legs as functions of the phase of the oscillators. Next, we design the local feedback controllers of the legs that use the nominal motions of the legs as reference signals. On the other hand, we determine the dynamic interactions among the nonlinear oscillators so that they interact with each other through the input signals from the touch sensors at the tips of the legs. The phase differences among the nonlinear oscillators emerge through the mutual entrainments of the oscillators. As a result, the proposed control system is expected to generate adequate and stable gait patterns corresponding to the dynamic states of the system or to the physical properties of the environment.

Control systems based on the bottom up approach design have already been applied to the locomotion of hexapod robots in some research. In such research, it has been shown that the control system can adaptively generate the adequate gait patterns corresponding to the system states or to the variations of the environment. The efficiency of the control system was also verified by hardware experiments [5]. On the other hand, it is difficult to design the control system of a quadruped locomotion robot which satisfies the dynamic stability of locomotion. Therefore, it is also difficult to design the control system which can autonomously generate the various gait patterns. There is only a small amount of research based on the bottom up approach that deals with the control system of a quadruped locomotion robot [6].

This paper deals with the design method of the control system of a quadruped locomotion robot based on the bottom up approach. The proposed control system has a hierarchical architecture. It is composed of the leg controller and the gait pattern controller. The leg controller drives the actuators of the legs by using local feedback control. The gait pattern controller involves non linear oscillators. Various gait patterns emerge through the mutual entrainment of these oscillators. The performance of the proposed control system is verified by numerical simulations and hardware experiments.

2 Equations of motion

Consider the quadruped locomotion robot shown in Fig. 1, which has four legs and a main body. Each leg is composed of two links which are connected to each other through a one DOF(degree of freedom) rotational joint. Each leg is connected to the main body through a one DOF rotational joint. The inertial and main body fixed coordinate systems are de-

finied as $[\mathbf{a}^{(-1)}] = [\mathbf{a}_1^{(-1)}, \mathbf{a}_2^{(-1)}, \mathbf{a}_3^{(-3)}]$ and $[\mathbf{a}^{(-1)}] = [\mathbf{a}_1^{(-1)}, \mathbf{a}_2^{(-1)}, \mathbf{a}_3^{(-3)}]$, respectively. $\mathbf{a}_1^{(-1)}$ and $\mathbf{a}_3^{(-1)}$ coincide with the nominal direction of locomotion and vertically upward direction, respectively. Each leg is enumerated from leg 1 to 4, as shown in Fig. 1. The joints of the leg are numbered as joint 1 and 2 from the main body toward the tip of the leg. We define $\theta_i^{(0)}$ ($i = 1, 2, 3$) as the components of Euler angle from $[\mathbf{a}^{(-1)}]$ to $[\mathbf{a}^{(0)}]$. We also define $\theta_j^{(i)}$ as the joint angle of link j of leg i . The rotational axis of joint j of leg i is parallel to the $\mathbf{a}_2^{(0)}$ axis. The following equations define the position vector from the origin of $[\mathbf{a}^{(-1)}]$ to that of $[\mathbf{a}^{(0)}]$.

$$\mathbf{r}^{(0)} = [\mathbf{a}^{(-1)}]r^{(0)} \quad (1)$$

$$r^{(0)} = [r_1^{(0)} r_2^{(0)} r_3^{(0)}]^T \quad (2)$$

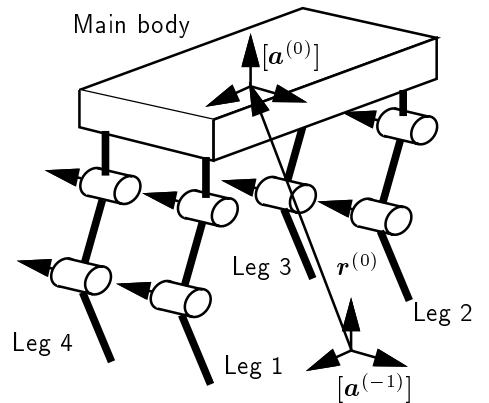


Fig. 1 Schematic model of a quadruped locomotion robot

The state variable is defined as follows;

$$q^T = \begin{bmatrix} \dot{r}_k^{(0)} & \omega_k^{(0)} & \dot{\theta}_j^{(i)} \end{bmatrix} \quad (3)$$

$(i = 1, \dots, 4), (j, k = 1, 2, 3)$

Equations of motion for state variable q are derived using Lagrangian formulation as follows;

$$M\ddot{q} + H(q, \dot{q}) = G + \sum(\tau_j^{(i)}) + \Lambda \quad (4)$$

where M is the generalized mass matrix and the term $M\ddot{q}$ expresses the inertia. $H(q, \dot{q})$ is the nonlinear term which includes Coriolis forces and centrifugal forces. G is the gravity term. $\sum(\tau_j^{(i)})$ is the input torque of the actuator at joint j of leg i . Λ is the reaction force from the ground at the point where the tip of the leg makes contact. We assume that there is no slip between the tips of the legs and the ground.

3 Gait pattern control

The architecture of the proposed control system is shown in Fig. 2. The control system is composed of the leg controllers and the gait pattern controller. The leg controllers drive all the joint actuators of the legs as to realize the desired motions that are generated by the gait pattern controller. The gait pattern controller involves non linear oscillators corresponding to each leg. The gait pattern controller receives the commanded signal of the nominal gait pattern as the reference. It also receives the feedback signals from the touch sensors at the tips of the legs. The generated gait pattern is determined by the phase differences between the non linear oscillators. A modified gait pattern is generated from the nominal gait pattern through the mutual entrainment of the oscillators with the feedback signals of the touch sensors. The generated gait pattern is given to the leg controller as the commanded signal of the locomotion pattern of the legs.

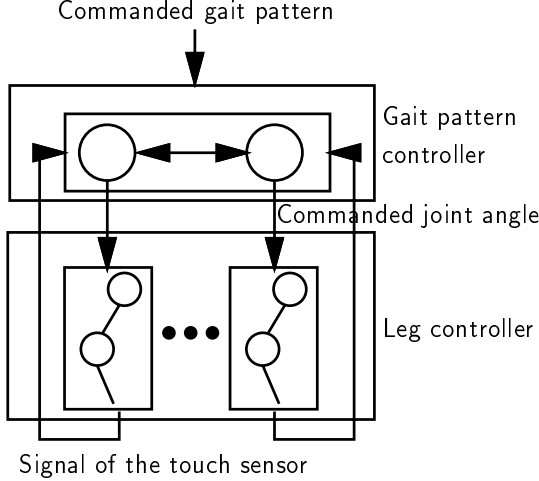


Fig. 2 Architecture of the proposed controller

3.1 Design of the gait

3.1.1 Design of trajectories of the legs

We determine two types of trajectories as the nominal trajectories of the tip of each leg. One is the trajectory for the swinging leg. The other is that for the supporting leg. The position of the tip of the leg where the transition from the swinging state to the supporting state occurs is called the anterior extreme position (AEP). Similarly, the position where the transition from the supporting state to the swinging state occurs is called the posterior extreme position (PEP). We determine the nominal trajectories which are expressed in the coordinate system $[\mathbf{a}^{(0)}]$ in the following way: First, we define the nominal PEP $\hat{r}_{eP}^{(i)}$ and the

nominal AEP $\hat{r}_{eA}^{(i)}$. The index $\hat{*}$ indicates the nominal value.

The trajectory for the swinging state is a closed curve given as the nominal trajectory $\hat{r}_{eF}^{(i)}$. This curve involves the points $\hat{r}_{eA}^{(i)}$ and $\hat{r}_{eP}^{(i)}$. On the other hand, the trajectory for the supporting state is a linear trajectory given as $\hat{r}_{eS}^{(i)}$. This linear trajectory also involves the points $\hat{r}_{eA}^{(i)}$ and $\hat{r}_{eP}^{(i)}$. These trajectories are given as functions of the phases of the oscillators. The state of the oscillator for leg i is expressed as follows;

$$z^{(i)} = \exp(j\phi^{(i)}) \quad (5)$$

where $z^{(i)}$ is a complex number which expresses the state of the oscillator, $\phi^{(i)}$ is the phase of the oscillator and j is the imaginary unit.

The nominal phase dynamics of the oscillator is defined as follows;

$$\dot{\hat{\phi}}^{(i)} = \omega \quad (6)$$

The nominal trajectories $\hat{r}_{eF}^{(i)}$ and $\hat{r}_{eS}^{(i)}$ are given as functions of the phase $\hat{\phi}^{(i)}$ of the oscillator.

$$\hat{r}_{eF}^{(i)} = \hat{r}_{eF}^{(i)}(\hat{\phi}^{(i)}) \quad (7)$$

$$\hat{r}_{eS}^{(i)} = \hat{r}_{eS}^{(i)}(\hat{\phi}^{(i)}) \quad (8)$$

We use one of these two trajectories alternatively at every step of AEP and PEP to generate the desired trajectory of the tip of the leg $\hat{r}_e^{(i)}(\hat{\phi}^{(i)})$.

$$\hat{r}_e^{(i)}(\hat{\phi}^{(i)}) = \begin{cases} \hat{r}_{eF}^{(i)}(\hat{\phi}^{(i)}) & 0 \leq \hat{\phi}^{(i)} < \hat{\phi}_A^{(i)} \\ \hat{r}_{eS}^{(i)}(\hat{\phi}^{(i)}) & \hat{\phi}_A^{(i)} \leq \hat{\phi}^{(i)} < 2\pi \end{cases} \quad (9)$$

The following relationships exist between AEP and PEP.

$$\hat{r}_{eP}^{(i)} = \hat{r}_{eF}^{(i)}(0) = \hat{r}_{eS}^{(i)}(0) \quad (10)$$

$$\hat{r}_{eA}^{(i)} = \hat{r}_{eF}^{(i)}(\hat{\phi}_A^{(i)}) = \hat{r}_{eS}^{(i)}(\hat{\phi}_A^{(i)}) \quad (11)$$

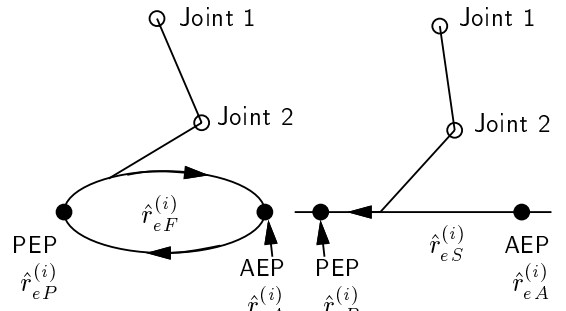


Fig. 3 Trajectory of the leg

Duty ratio $\hat{\beta}^{(i)}$ for leg i is defined to represent the ratio between the nominal time for the supporting state and the period of one cycle of the nominal locomotion.

$$\hat{\beta}^{(i)} = 1 - \frac{\hat{\phi}_A^{(i)}}{2\pi} \quad (12)$$

The nominal stride of leg i is given as follows;

$$\hat{S}^{(i)} = \hat{r}_{eA}^{(i)} - \hat{r}_{eP}^{(i)} \quad (13)$$

3.1.2 Design of the gait pattern

There are three gait patterns in which two legs support the main body at any instant during locomotion: In the trot pattern legs 1 and 3 form one pair and legs 2 and 4 form the other pair, in the pace pattern legs 1 and 2 form one pair and legs 3 and 4 form the other pair, finally in the bounce pattern legs 1 and 4 form one pair and legs 2 and 3 form the other pair. The following relationships exist among the phase variables of the periodic motions of the legs.

$$\text{Trot} : \hat{\phi}^{(1)} = \hat{\phi}^{(3)}, \hat{\phi}^{(2)} = \hat{\phi}^{(4)} \quad (14)$$

$$\text{Pace} : \hat{\phi}^{(1)} = \hat{\phi}^{(2)}, \hat{\phi}^{(3)} = \hat{\phi}^{(4)} \quad (15)$$

$$\text{Bounce} : \hat{\phi}^{(1)} = \hat{\phi}^{(4)}, \hat{\phi}^{(2)} = \hat{\phi}^{(3)} \quad (16)$$

As can be seen from equations (14) ~ (16), phases of the pairs of oscillators are coupled and the phase differences between them are zero.

A shift of the phase differences between the coupled oscillators by $\frac{\pi}{2}$ causes the gait pattern to change from those explained above to the walk pattern (Fig. 4). For example, the phase shift $\frac{\pi}{2}$ of the trot pattern produces another pattern in which the legs 1,3,2 and 4 touch on the ground in this order. This modified pattern is called *transverse walk*.

In this paper, we consider the gait control method which makes a transition from the trot pattern to walk (or vice versa) by using an external commanded signal.

Trot pattern and walk pattern can be written as follows;

$$\phi^{(i+2)} = \phi^{(i)} + \Gamma^{(m)} \quad (i = 1, 2) \quad (17)$$

$$\Gamma^{(m)} = \begin{cases} 0 & \text{Trot} \quad (m = 2) \\ 2\pi(1 - \hat{\beta}) & \text{Walk} \quad (m = 1) \end{cases}$$

The gait pattern is designed based on Eq.(17).

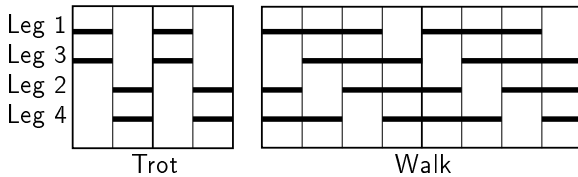


Fig.4. The trot and walk patterns

3.2 Motion control

3.2.1 Leg controller

The angle of joint j of leg i is derived from the geometrical relationship between the trajectory $\hat{r}_e^{(i)}(\hat{\phi}^{(i)})$ and the joint angle. $\hat{\theta}_j^{(i)}$ is written as a function of phase $\hat{\phi}^{(i)}$ as follows;

$$\hat{\theta}_j^{(i)} = \hat{\theta}_j^{(i)}(\hat{\phi}^{(i)}) \quad (18)$$

The commanded torque at each joint of the leg is obtained by using local PD feedback control as follows;

$$\tau_j^{(i)} = K_{Pj}(\hat{\theta}_j^{(i)} - \theta_j^{(i)}) + K_{Dj}(\dot{\hat{\theta}}_j^{(i)} - \dot{\theta}_j^{(i)}) \quad (19)$$

$(i = 1, \dots, 4, j = 1, \dots, 3)$

where $\tau_j^{(i)}$ is the actuator torque at joint j of leg i , and K_{Pj}, K_{Dj} are the feedback gains, the values of which are common to all joints in all legs.

3.2.2 Gait pattern controller

We design the phase dynamics of the oscillators corresponding to each leg as follows;

$$\dot{\phi}^{(i)} = \omega + g_1^{(i)} + g_2^{(2)} \quad (i = 1, \dots, 4) \quad (20)$$

where $g_1^{(i)}$ is the term which is derived from the nominal gait pattern and $g_2^{(i)}$ is the term caused by the feedback signal of the touch sensors of the legs.

Function $g_1^{(i)}$ is designed in the following way: We define the following potential function.

$$V(\phi^{(i)}, \Gamma^{(m)}) = K \sum_{i=1}^2 \left(\phi^{(i)} - \phi^{(i+2)} - \Gamma^{(m)} \right)^2 \quad (21)$$

where parameter $\Gamma^{(m)}$ represents the nominal gait pattern defined in Eq.(17) and is given as a commanded signal.

Function $g_1^{(i)}$ is derived from the potential function V as follows;

$$g_1^{(i)} = - \frac{\partial V(\phi^{(i)}, \Gamma^{(m)})}{\partial \phi^{(i)}} = -K \left(\phi^{(i)} - \phi^{(i+2)} - \Gamma^{(m)} \right) \quad (22)$$

Function $g_2^{(i)}$ is designed in the following way: First, we consider the pair of legs i, j ($i = 1, j = 3$ or $i = 2, j = 4$). Suppose that leg i is in the swinging state and leg j is in the supporting state. The transition of these states occurs at the instant when the swinging leg touches the ground. Suppose that

$\phi_A^{(i)}$, $\phi_P^{(j)}$ are the phases of leg i and leg j at the instant when leg i touches on the ground, respectively. Similarly, $r_{eA}^{(i)}$, $r_{eP}^{(j)}$ are the positions of leg i and leg j at that instance, respectively. When leg i touches the ground, the following procedure is needed.

1. The phase of the oscillator for leg i is changed from $\phi_A^{(i)}$ to $\hat{\phi}_A^{(i)}$. On the other hand, the phase of the oscillator for leg j is changed from $\phi_P^{(j)}$ to 0.
2. Alter the nominal trajectory of the tip of leg i from the swinging trajectory $\hat{r}_{eF}^{(i)}$ to the supporting trajectory $\hat{r}_{eS}^{(i)}$.
3. Replace parameter $\hat{r}_{eA}^{(i)}$, that is one of the parameters of the nominal trajectory $\hat{r}_{eS}^{(i)}$, with $r_{eA}^{(i)}$.
4. Change the nominal trajectory of the tip of leg j from the supporting trajectory $\hat{r}_{eS}^{(j)}$ to the swinging trajectory $\hat{r}_{eF}^{(j)}$. Also replace parameter $\hat{r}_{eP}^{(j)}$, that is one of the parameters of the nominal trajectory $\hat{r}_{eS}^{(j)}$, with $r_{eP}^{(j)}$.

Function $g_2^{(i)}$ is given as follows;

$$\begin{aligned} g_2^{(i)} &= \hat{\phi}_A^{(i)} - \phi_A^{(i)} && \text{at the instant leg } i \\ &&& \text{touches the ground} \\ g_2^{(j)} &= -\phi_P^{(j)} && \text{at the instant leg } j \\ &&& \text{takes off from the ground} \end{aligned} \quad (23)$$

The pair of oscillators form a dynamic system that affect each other through two types of interactions. One is continuous interactions derived from the potential function V which depends on the nominal gait pattern. The other is the pulse-like interactions caused by the feedback signals from the touch sensor. Through these interactions, the oscillators generate gait patterns that satisfy the requirements of the environment.

4 Stability analysis of motion

The steady locomotion of the quadruped locomotion robot is strictly periodic and is characterized by a limit cycle in the state space. In this section, the analysis of the stability of the limit cycle in the steady locomotion of the quadruped locomotion robot is described.

The stability of the limit cycle is examined in the following way: First, four variables are selected as state variables.

$$X \in R^4, \quad X = \begin{bmatrix} \theta_1^{(0)} & \theta_2^{(0)} & \dot{\theta}_1^{(0)} & \dot{\theta}_2^{(0)} \end{bmatrix} \quad (24)$$

When the robot starts the locomotion under a certain initial condition, the variable set X moves on a

certain trajectory in the four-dimensional state space. If we choose a Poincaré section using the timing when the tip of a leg touches the ground, the first intersection of the trajectory of X with the Poincaré section is mapped as X_0 , and for every intersection, the corresponding values of X lead to a sequence of iterates in the state space.

$$X_1 \quad X_2 \quad \cdots \quad X_n \quad \cdots$$

The Poincaré map from X_n to X_{n+1} is expressed as follows;

$$X_{n+1} = F(X_n) \quad (25)$$

The fixed point \hat{X} is defined if \hat{X} satisfies the following equation on the Poincaré section.

$$\hat{X} = F(\hat{X}) \quad (26)$$

This Poincaré map is approximated by use of linearization around the fixed point.

$$X_{n+1} - \hat{X} = M(X_n - \hat{X}) \quad (27)$$

The necessary condition for the asymptotic stability of the sequence of points $\{X_n\}$ is that all of the eigen values of matrix M are smaller than one in magnitude, λ_k ($k = 1, \dots, 4$) $|\lambda_k| < 1$.

5 Numerical simulation

Table 1 shows the physical parameters of the robot which are used in numerical simulations.

Table 1

Main body		
Width	0.182	[m]
Length	0.338	[m]
Height	0.05	[m]
Momentum of inertia (x)	0.010	[kgm ²]
Momentum of inertia (y)	0.046	[kgm ²]
Momentum of inertia (z)	0.046	[kgm ²]
Legs		
Length of link 1	0.026	[m]
Length of link 2	0.188	[m]
Length of link 3	0.193	[m]
Mass of link 1	0.320	[kg]
Mass of link 2	0.918	[kg]
Mass of link 3	0.595	[kg]
Momentum of inertia of link 1	1.0E-06	[kgm ²]
Momentum of inertia of link 2	1.8E-02	[kgm ²]
Momentum of inertia of link 3	5.1E-03	[kgm ²]

Numerical simulations are implemented under the condition that the nominal stride \hat{S} and the nominal gait pattern are fixed. The nominal duty ratio $\hat{\beta}$ is

selected as a parameter. The dynamic stability of each gait pattern depends on the value $\hat{\beta}$. For example, for $\hat{\beta} = 0.5$, trot, pace and bounce patterns are the most stable dynamically, whereas for $\hat{\beta} = 0.75$ the walk pattern is stable.

The trajectory of the tip of the leg is given as follows;

$$r_{eS1}^{(i)} = \frac{S}{\phi_A^{(i)}}(\phi^{(i)} - \cos \phi^{(i)}) + r_{eP1}^{(i)} \quad (28)$$

$$r_{eS2}^{(i)} = \frac{S}{\phi_A^{(i)}}(1 - \sin \phi^{(i)}) + r_{eP2}^{(i)} \quad (29)$$

$$r_{eF1}^{(i)} = \frac{S}{2\pi - \phi_A^{(i)}}(\phi^{(i)} - \phi_A^{(i)}) + r_{eA1}^{(i)} \quad (30)$$

$$r_{eF2}^{(i)} = \frac{S}{2\pi - \phi_A^{(i)}}(\phi^{(i)} - \phi_A^{(i)}) + r_{eA2}^{(i)} \quad (31)$$

The nominal time period of the swinging state is chosen as 0.20 [sec]. The frequency band width of joint 1, 2 and 3 are given as 50.0 [Hz], 5.5 [Hz], 9.5 [Hz] for feedback gains of the joints, respectively. Numerical simulations are implemented for the walk pattern and trot pattern.

In order to compare the performance of the proposed control system, another control system is simulated in which the leg controller drives the legs as to follow the nominal trajectories using local feedback control. Two cases are examined by numerical simulations: One is the case where the controller uses a fixed gait pattern and the nominal trajectories as the desired trajectories (CASE 1). The other is the case where the controller also uses a fixed gait pattern but the controller is the proposed one that is explained in Section 3 (CASE 2).

Figure 5 shows the result of the stability analysis where we checked the motion of the robot. It is performed by using the method introduced in Section 4, based on the simulation results. It can be seen that the proposed control system has better performance compared with the control system that uses the nominal trajectories as the desired trajectories. The proposed control system established stable locomotion of the robot with a wide parameter variance for duty ratio $\hat{\beta}$.

Figure 6 shows the gait pattern obtained as the simulation result of CASE 1. From these figures, it can be seen that if $\hat{\beta}$ is varied excessively, instability occurs in the fixed gait pattern. For the case where the walk pattern is being commanded, if $\hat{\beta}$ is decreased to 0.5 an unstable and irrhythmic pattern is promoted (Fig. 6.a). Similarly, for the case where the trot pattern is being commanded, if $\hat{\beta}$ is increased to 0.75 the gait pattern is still that of trot (Fig. 6.d). The reason of the instability is that the control system of CASE 1

cannot modify the gait patterns adaptively to the variations in the locomotion velocities.

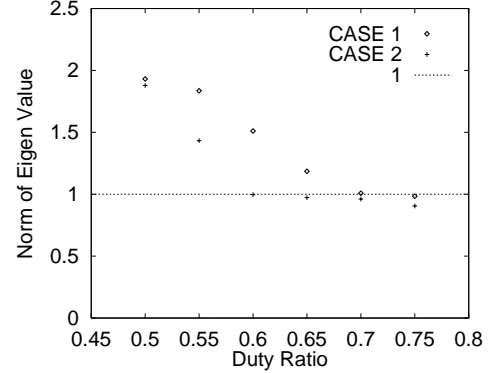


Fig. 5.a Stability in the walk pattern

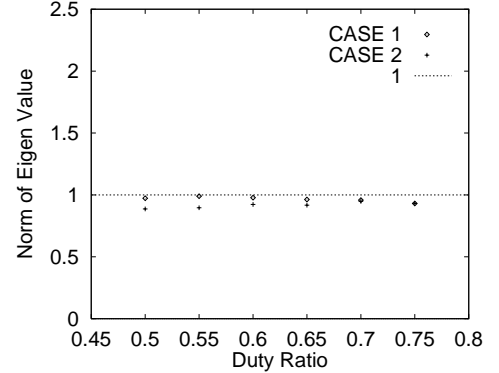


Fig. 5.b Stability in the trot pattern

CASE 1: Walk

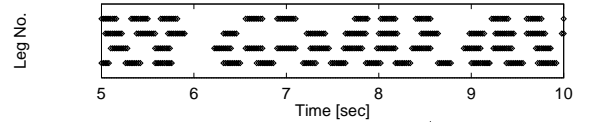


Fig. 6.a Gait pattern diagram($\hat{\beta} = 0.50$)

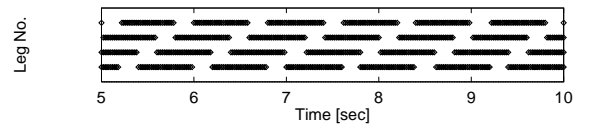


Fig. 6.b Gait pattern diagram($\hat{\beta} = 0.75$)

Trot

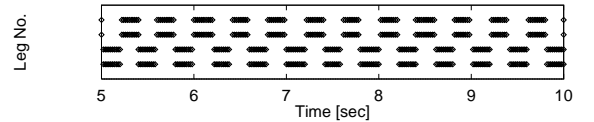


Fig. 6.c Gait pattern diagram($\hat{\beta} = 0.50$)

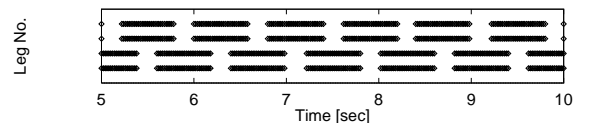


Fig. 6.d Gait pattern diagram($\hat{\beta} = 0.75$)

Figure 7 shows the gait pattern obtained from the simulation result of CASE 2. By varying the duty ratio, the appropriate gait pattern emerges. This is especially evident in Fig. 7.d where the trot pattern is being commanded but $\hat{\beta} = 0.75$. The most stable gait pattern for this duty ratio, the walk pattern emerges. Figure 8 indicates the correlation coefficients among the motion of the legs which are calculated from the results of the simulations where the walk pattern is commanded(Fig. 8.a) and the trot pattern is commanded(Fig. 8.b). The correlation coefficients are given in Eq.(32), which characterize the relationships among the motion of the legs.

From these figures, two results are derived. The first one is that both Fig. 8.a and Fig. 8.b show a similar trend. This means that the controller behaves in a similar fashion regardless of the commanded pattern. The second result is that the correlation coefficient degrades as duty ratio $\hat{\beta}$ increases. However, it is known that an increase in $\hat{\beta}$ implies a decrease in the velocity of locomotion and vice versa. This means, therefore, that the control system modifies the commanded nominal gait pattern adaptively, corresponding to the locomotion velocity and it also preserves the dynamic stability of locomotion. As a result, if the walk pattern is commanded but a high velocity is desired, the control system changes the gait pattern from walk to trot autonomously. The reverse is also true; if the trot pattern is commanded but a slow velocity of locomotion is desired, the walk pattern is generated.

$$\zeta_i = \begin{cases} 0 & \text{Supporting state} \\ 1 & \text{Swinging state} \end{cases}$$

$$W_{ii+2} = \frac{\int \zeta_i \zeta_{i+2} dt}{\sqrt{\int \zeta_i dt} \sqrt{\int \zeta_{i+2} dt}} \quad (i = 1, 2) \quad (32)$$

CASE 2:
Walk

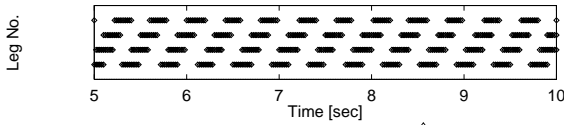


Fig. 7.a Gait pattern diagram($\hat{\beta} = 0.50$)

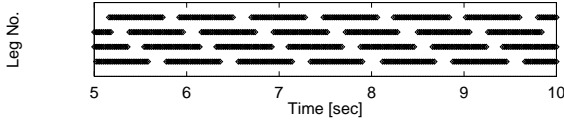


Fig. 7.b Gait pattern diagram($\hat{\beta} = 0.75$)

Trot

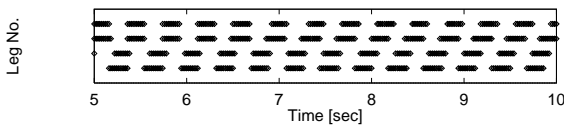


Fig. 7.c Gait pattern diagram($\hat{\beta} = 0.50$)

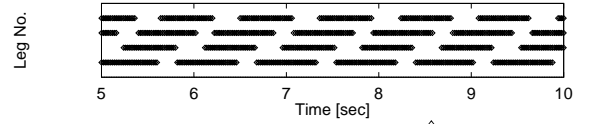


Fig. 7.d Gait pattern diagram($\hat{\beta} = 0.75$)

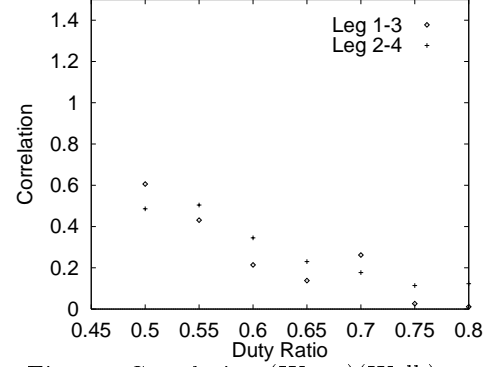


Fig. 8.a Correlation (W_{ii+2})(Walk)

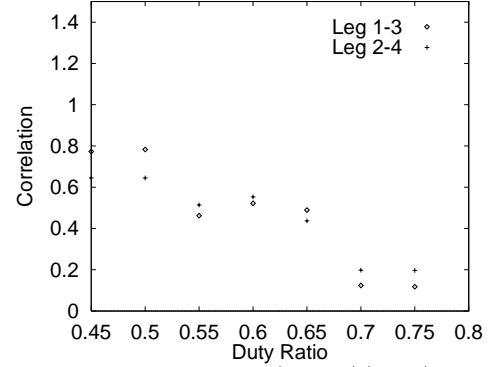


Fig. 8.b Correlation (W_{ii+2})(Trot)

6 Hardware experiments

A picture of the hardware equipment is shown in Fig. 9.



Fig. 9 The hardware equipment

The architecture of the hardware equipment is shown in Fig. 10.

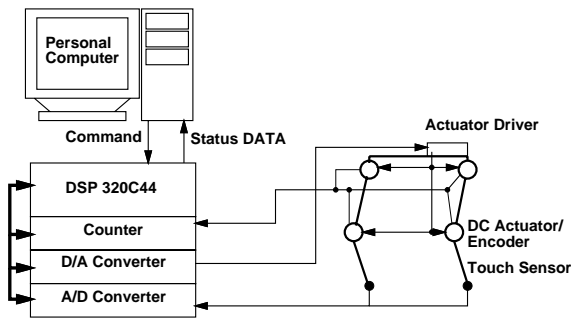


Fig. 10 The architecture of the hardware equipment

The performance of the proposed control system was verified by hardware experiments. Figures 11.a and 11.b show the effect of duty ratio $\hat{\beta}$ when the walk pattern is commanded, and Figs. 12.a and 12.b show the same, in hardware experiments. From these figures, we can see that the proposed control system has a good robustness and adaptability.

Walk

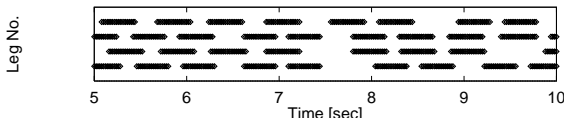


Fig. 11.a Gait pattern diagram($\hat{\beta} = 0.65$) (Walk)

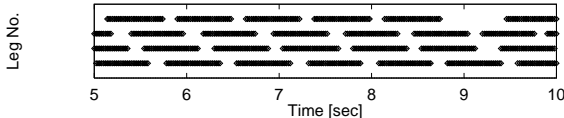


Fig. 11.b Gait pattern diagram($\hat{\beta} = 0.75$) (Walk)

Trot

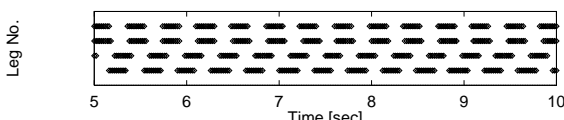


Fig. 12.a Gait pattern diagram($\hat{\beta} = 0.50$) (Trot)

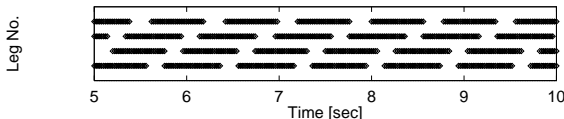


Fig. 12.b Gait pattern diagram($\hat{\beta} = 0.75$) (Trot)

7 Conclusions

We proposed a control system with a hierarchical architecture which is composed of the leg controller and the gait pattern controller. The leg controller drives the actuators at the joints of the legs by use of high-gain local feedback based on the commanded signal from the gait pattern controller. Whereas the gait pattern controller alternates the motion primitives synchronizing with the signals from the touch

sensors at the tips of the legs, and stabilizes the phase differences among the motions of the legs adaptively. The performance of the proposed control system was verified by numerical simulations and hardware experiments.

Acknowledgments

The authors were funded by grants from the The Japan Society for the Promotion of Science (JSPS) as the Research for the Future program (RFTF) and from the Japan Science and Technology Corporation (JST) as the Core Research for Evolutional Science and Technology program (CREST).

References

- [1] T. Mita and T. Ikeda, "Proposal of a Variable Constraint Control for SMS with Application to a Running and Quadruped," Proc. of the 1999 IEEE International Conference on System, Man and Cybernetics, III, pp.140-145, (1999)
- [2] H. Cruse, C. Bartling, J. Dean, T. Kindermann, J. Schmitz, M. Schumm and H. Wagner, "Coordination in a Six-legged Walking system: Simple solutions to complex problems by exploitation of physical properties," From Animals to Animats, pp.84-93, (1996)
- [3] G.M.Nelson, R.D.Quinn, R.J.Bachmann and W.C.Flannigan, "Design and Simulation of a Cockroach-like Hexapod Robot," Proc. 1997 IEEE International Conference on Robotics and Automation, No.2, pp.1106-1111, (1997)
- [4] G.M.Nelson and R.D.Quinn, "Posture Control of a Cockroach-like Robot," Proc. of the 1998 IEEE International Conference on Robotics and Automation, Vo.1, pp.157-162, (1998)
- [5] K. Akimoto, S. Watanabe and M. Yano, "A insect robot controlled by the emergence of gait patterns," Proc. of International Symposium on Artificial Life and Robotics, Vol.3, No.2, pp.102-105, (1999)
- [6] H.Kimura, K.Sakaura and S.Akiyama, "Dynamic Walking and Running of the Quadruped Using Neural Oscillator," Proc. IROS, Vol.1, pp.50-57, (1998)
- [7] M.J.Coleman, M.Garcia, A.L.Ruina and J.S.Camp and A.Chatterjee, "Stability and Chaos in Passive-Dynamic Locomotion," Solid Mechanics and its Applications, Vol.63, pp.407-416, (1997)